Extended Abstracts of the 1995 International Conference on Solid State Devices and Materials, Osaka, 1995, pp. 995-997



# Superior Detectivity of (111) GaAs/AlGaAs p-Type QW Infrared Photodetector

Taehee Cho, Hyungsuk Kim, Songcheol Hong and Youngse Kwon

*Opto-Electronics Research Center Department of Electrical Engineering*
*Korea Advanced Institute of Science and Technology, Taejon, 305-701, Korea*

Intersubband absorptions in p-type GaAs/$Al_{0.3}Ga_{0.7}As$ quantum well (QW) grown on (111) substrates are theoretically investigated with multiband effective-mass model. Because of the stronger band mixing of (100) QW, the peak absorption coefficient of (100) QW is ~2 times as large as that of (111) QW. Nevertheless, the detectivity of (111) QW is found to be ~30% larger than that of (100) QW because of the smaller dark current of (111) QW. This is due to the smaller heavy-hole confinement energy in (111) QW.

## 1. INTRODUCTION

Intersubband transitions in a quantum well (QW) have been of recent interest, especially for far-infrared photodetector application. The detection of long wavelength radiation in 7 - 14 $\mu$m range has numerous applications.[1] Traditionally band to band spectra in HgCdTe and other small bandgap materials are used in semiconductor detectors.[2] However, the same material properties that yield small bandgaps which are often also produce a soft material which is difficult to grow and process. This has led to increased interest in interband absorption in multiple quantum well structures. Since, in n-type quantum well infrared photodetector (QWIP), the absorption of normal incident light is forbidden by selection rule[3], complicate fabrication steps are involved to develo[illegible]rays. P-type multiple quantum well has been examined for normal incident photodetector because the mixing of heavy hole and light hole states enables the transitions which are not allowed by the selection rules.[1,4] The intervalence band transitions of (100) QWs have been extensively studied both theoretically and experimentally.[1,4] However, little attention has been paid to quantization direction other than [100] because it is usually difficult to prepare a high quality QW structures.[5-8] Thesedays the epitaxial growth of high quality GaAs/AlGaAs QWs on (111) substrate has been succeeded.[9] We presented the first theoretical results on the responsivity and detectivity of QWIP based on intervalence band transitions in (111) QWs.

The intersubband transitions and responsivity in (111) QW are studied by using (2×2) multiband effective mass model and compared with those of (100) QW. Also the dark current of QWIP is estimated by hot carrier temperature model[10] and the detectivity are obtained from these calculations.

## 2. ANALYSIS

The structure of QWIP considered here consists of p-type 40 Å GaAs /$Al_{0.3}Ga_{0.7}As$ QW. The hole subbands in (100) and (111) QWs are obtained by solving the different Hamiltonians.[11] The material parameters used in this calculation at 80 K are : $E_g$=1.51+1.62$x$ eV[12,13],

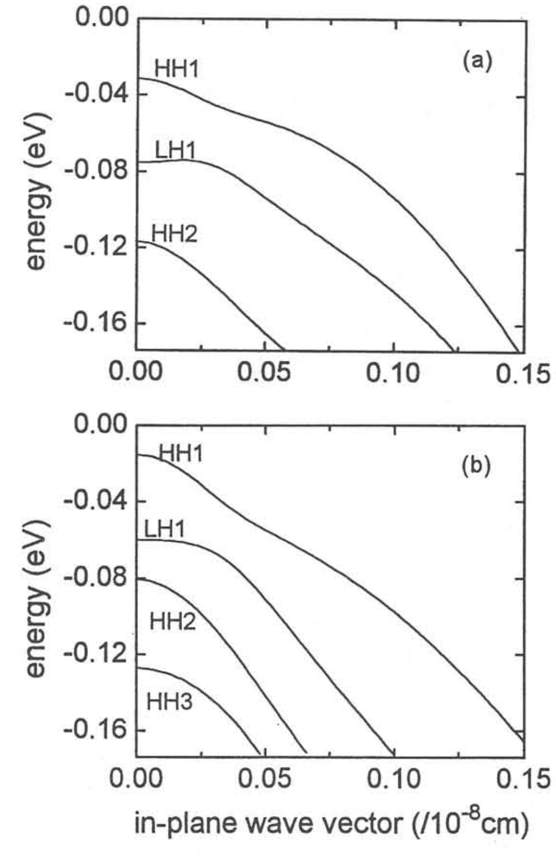


Fig. 1. Hole band structures of GaAs/$Al_{0.3}Ga_{0.7}As$ QW with 40 Å well width. (a) is for the (100) QW and (b) for the (111) QW. The band offset is 174 (meV).

$\Delta E_v$=0.580$x$ eV[14], where $x$ is Al mole fraction of the barrier. Figure 1 shows the hole bandstructure of (100) and (111) QWs. The separation between ground heavy-hole and light-hole states, E(HH1) − E(LH1), is larger in the (111) QW. This large separation reduces band mixing and yields smaller in-plane heavy-hole mass, which reduces the density of states of the heavy-hole band.[11] As a result, the separation between the Fermi level and the ground heavy-hole state energy is larger in the (111) QW at the same hole concentration. The energy separations are 3 and 10 meV in the (100) QW and the (111)

QW, respectively. However the Fermi level is located at the lower energy in the (111) QW since the difference of ground heavy-hole state energy of the (100) QW and the (111) QW is larger than the separation. At the hole concentration of $2\times10^{18}$ cm$^{-2}$, the Fermi levels in the (100) and the (111) QWs are located at -34 and - 26 meV from the top of bulk valence band, respectively.

The absorption coefficient of intervalence band transitions between subband n and n$'$ is given by[15]

$$\alpha_{nn'}(\omega) = \frac{4\pi^2 e^2}{\epsilon m_0^2 \omega c} \times \sum_{k_\parallel} [f_n(k_\parallel) - f_{n'}(k_\parallel)] |\hat{\varepsilon} \cdot P_{nn'}(k_\parallel)|^2$$

$$\times \frac{1}{\pi} \frac{\tau/\hbar}{[|E_{n'}(k_\parallel) - E_n(k_\parallel)| - \hbar\omega]^2 + [\tau/\hbar]^2}, \quad (1)$$

where $\epsilon$ is the dielectric constant, $m_0$ is the free electron mass, $E_n(k_\parallel)$ is the hole subband $n$, $P_{nn'}(k_\parallel)$ is the momentum matrix element, $f_n(k_\parallel)$ is the carrier distribution function associated with subband $n$, and $\tau/\hbar$ is the broadening energy. In this calculation the broadening of 8 meV was assumed. The momentum matrix elements of a (111) QW are derived and described as

$$\hat{e} \cdot P_{nn'} = \hbar \hat{e} \cdot \sum_{\nu,\nu'} \left( P_{\nu\nu'} O_{\nu\nu'}^{nn'} + Q_{\nu\nu'} D_{\nu\nu'}^{nn'} \right), \quad (2)$$

where $\hat{e} \cdot P_{\nu\nu'}$ and $\hat{e} \cdot Q_{\nu\nu'}$ are the matrix elements of the $4 \times 4$ matrices. They are written in the form

$$\begin{pmatrix} A_1 & B & C & 0 \\ B^* & A_2 & 0 & C \\ C^* & 0 & A_2 & -B \\ 0 & C^* & -B^* & A_1 \end{pmatrix} \quad (3)$$

with the coefficients $A_1$, $A_2$, $B$, and $C$ are given in Table I for (100) QW and (111) QW in terms of the Luttinger parameters $\gamma_1$, $\gamma_2$, $\gamma_3$, and wavevector $k_1$, $k_2$. $O_{\nu\nu'}^{nn'}$ and $D_{\nu\nu'}^{nn'}$ are elements of the overlap matrix and the dipole matrix.[14]

For QWIP applications, transitions to states close to barrier height are useful because the excited carriers must be collected to be an electrical signal. Figure 2 shows the normalized absorption coefficients of the (100) and the (111) QWs at T=80 K. The absorption peaks due to HH1 $\leftrightarrow$ extended states appear near 0.15 eV ($\sim 8$ $\mu$m) and 0.16 eV in the (100) QW and in the (111) QW, respectively.

Oscillator strengths between subbands are larger in a (100) QW than in a (111) QW because of the stronger band mixing. Joint density of states of HH1 $\leftrightarrow$ extended states is larger in the (100) QW since the effective mass difference between ground heavy-hole state and extended states is smaller than in the (111) QW. These are the two major reason why absorption coefficient is larger in the (100) QW. Responsivity can be simply written as R= $(e/\hbar\omega)\eta g$,[3] where $e$ is the electronic charge, $\hbar\omega$ is the photon energy of the light source, $\eta$ is the quantum efficiency and $g$ is the photoconductive gain. $\eta = 1 - exp(-2\alpha l)$, where $\alpha$ is absorption coefficient and $l$ is total well width. If $\alpha \times l$ is small, quantum

Table I. Coefficients of in-plane elements defining the matrices $\hat{e} \cdot P$ and $\hat{e} \cdot Q$ (a) for (100) QW and (b) for (111) QW.

(a)

| | $\hat{e_\parallel} \cdot P$ | $\hat{e_\parallel} \cdot Q$ |
|---|---|---|
| $A_1$ | $-(\gamma_1 + \gamma_2)k_1$ | 0 |
| $A_2$ | $-(\gamma_1 - \gamma_2)k_1$ | 0 |
| $B$ | 0 | $i2\sqrt{3}\gamma_3$ |
| $C$ | $-\sqrt{3}\gamma_2 k_1 + i2\sqrt{3}\gamma_3 k_3$ | 0 |

$k_1 \rightarrow [100], k_2 \rightarrow [010], k_3 \rightarrow [001]$

(b)

| | $\hat{e_\parallel} \cdot P$ | $\hat{e_\parallel} \cdot Q$ |
|---|---|---|
| $A_1$ | $-(\gamma_1 + \gamma_3)k_1$ | 0 |
| $A_2$ | $-(\gamma_1 - \gamma_3)k_1$ | 0 |
| $B$ | $-\frac{2(\gamma_2-\gamma_3)}{\sqrt{6}}k_1 - i\frac{4(\gamma_2-\gamma_3)}{\sqrt{6}}k_2$ | $\frac{2(2\gamma_2+\gamma_3)}{\sqrt{3}}$ |
| $C$ | $-\frac{\gamma_2+2\gamma_3}{\sqrt{3}}k_1 + i\frac{2(\gamma_2+2\gamma_3)}{\sqrt{3}}k_2$ | $\frac{4(\gamma_2-\gamma_3)}{\sqrt{6}}$ |

$k_1 \rightarrow [11\bar{2}], k_2 \rightarrow [\bar{1}10], k_3 \rightarrow [111]$

efficiency is directly proportional to absorption coefficient and so is responsivity. The quantum efficiencies are 38% and 25% for the (100) QW and the (111) QW, respectively. Photoconductive gain is function of applied electrical field. R of (111) QW to R of (100) QW ratio is 70%.

The detectivity of a photodetector can be estimated by the simple equation D*=$R_p\sqrt{A}/i_n$,[1] where $R_p$ is peak responsivity, A is detetctor area and $i_n = \sqrt{4eI_d g\Delta f}$ is noise current of a photodetector. Dark current $I_d$ can be written as [1]

$$J_{dark} = e[v_{dhh} \int D_{hh} f_0 dE + v_{dlh} \int D_{lh} f_0 dE], \quad (4)$$

where $v_{dhh}$ and $v_{dlh}$ are the heavy-hole drift velocity and light-hole drift velocity, respectively, and $D_{hh}$ and $D_{lh}$ are the density of states of heavy-hole state and light-hole state in the continuum along the growth direction, respectively. The energy-distribution function[10] $f_0 = 1/(1 + exp((E - E_{fc})/kT_c))$ is determined by hot carrier temperature $T_c$ and quasi-Fermi level of extended states. Since quasi-Fermi level of the (111) QW is located at lower energy than that of the (100) QW, the dark current of (111) QW is smaller. In our calculation, we only consider small bias range. The high bias cause to saturate responsivity and the dark current is increased rapidly with bias in the high bias range. The dark current of (100) QW and (111) QW with biased electric field are showed in Fig. 3. The calculated detecdivity are $1\times10^{10}$ and $1.3\times10^{10}$ cm$\sqrt{Hz}$/W in the (100) QW and the (111) QW, respectively, for $\mathcal{E}$=1 kV/cm and T=80 K.

## 3. CONCLUSION

In conclusion, we compared the performances of the (100) p-QWIP and the (111) p-QWIP for the first time. The (111) p-QWIP has the smaller infrared absorption

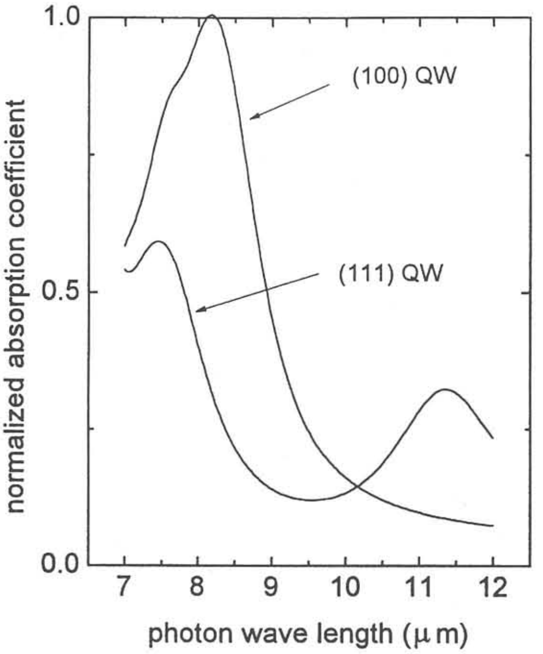


Fig. 2. Absorption coefficients of the intervalence band transitions in (100) QW and (111) QW with 40 Å well width at 80 K. The absorption due to HH1 $\leftrightarrow$ extended states is larger in the (100) QW at wavelength $\sim 8\ \mu m$ and in the (111) QW at wavelength $\sim 11\ \mu m$. The absorption peak of the (111) QW at wavelength $\sim 11\ \mu m$ is due to bound-to-bound transition.

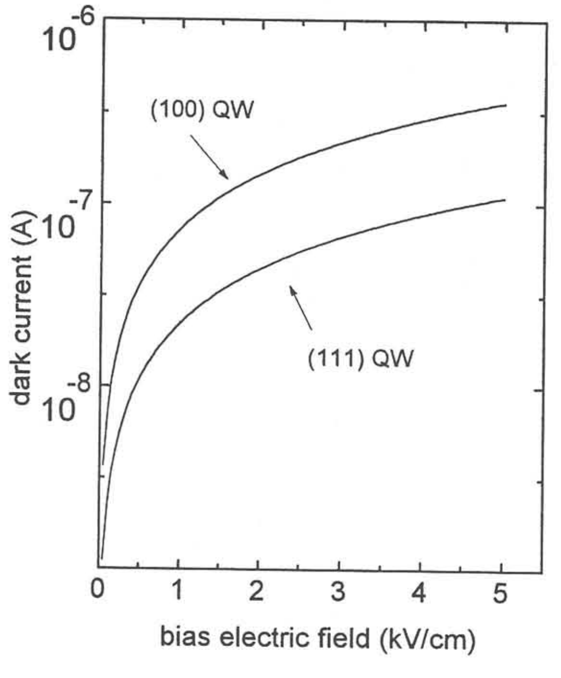


Fig. 3. Dark current vs bias electric field for the (100) QW and (111) QW with 40 Å well width at 80 K.

coefficient than the (100) p-QWIP. Nevertheless, detectivity of the (111) QW is ~30% larger than that of the (100) QW because extremly low dark current. Considering the storage capacity of read-out circuit, (111) p-QWIP may be an atrractive candidate for QWIP applications.

## Acknowledgement

This work is partially supported by Korea Science and Engineering Foundation, OERC-94-02-03-01.

## References

1) B. F. Levine, S. D. Gunapala, J. M. Kuo, S. S. Pei, and S. Hui, Appl. Phys. Lett. **59** (1991) 1864.

2) P. Man and D. S. Pan, Phys. Rev. B **44** (1991) 8745.

3) L. C. West and S. J. Eglash, Appl. Phys. Lett. **46** (1985) 1156

4) P. Man and D. S. Pan, Appl. Phys. Lett, **61** (1992) 2799

5) A. Y. Cho, J. Appl. Phys. **41** (1970) 2780

6) W. I. Wang, J. Vac. Sci. Technol. B **1** (1983) 630

7) S. Subbanna, H. Kroemer, and J. L. Merz, J. Appl. Phys. **59** (1986) 488.

8) T. Fukunaga, T. Takamori, and H. Nakashima, J. Cryst. Growth **85** (1987) 81.

9) T. Hayakawa, M. Kondo, T. Suyama, K. Takahashi, S. Yamamoto, and T. Hijikata, Jpn. J. Appl. Phys. Pt. 2 **26** (1987) L 302.

10) P. Man and D. S. Pan, Appl. Phys. Lett. **66** (1995) 194.

11) E. P. O'Reilly and A Ghiti: *QUANTUM WELL LASERS*, eds. P. S. Zory, Jr. (Academic, London, 1986), p. 342.

12) J. S. Blakemore, J. Appl. Phys. **53** (1982) R 123.

13) B. Monemar, Phys. Rev. B **8** (1973) 5711.

14) J. Batey and S. L. Wright, Appl. Phys. Lett. **59** (1986) 200.

15) Y. C. Chang and R. B. James, Phys. Rev. B **39** (1989) 12672.